

SYK inhibition and response prediction in diffuse large B-cell lymphoma

Shuhua Cheng,¹ Greg Coffey,² X. Hannah Zhang,¹ Rita Shaknovich,¹ Zibo Song,¹ Pin Lu,¹ Anjali Pandey,² Ari M. Melnick,³ Uma Sinha,² and Y. Lynn Wang¹

¹Department of Pathology and Laboratory Medicine, Weill Cornell Medical College, New York, NY; ²Portola Pharmaceuticals Inc, South San Francisco, CA; and ³Department of Medicine, Weill Cornell Medical College, New York, NY

Diffuse large B-cell lymphoma (DLBCL) is the most common type of non-Hodgkin lymphoma, and the role of SYK in its pathogenesis is not completely understood. Using tissue microarray, we demonstrated for the first time that SYK protein is activated in 27 of 61 (44%) primary human DLBCL tissues. Among DLBCL cell lines, 7 were sensitive and 3 were resistant to a highly specific SYK inhibitor, PRT060318. In sensitive DLBCL cells, SYK inhibition blocked the G₁-S transi-

tion and caused cell-cycle arrest. This effect was reproduced by genetic reduction of SYK using siRNA. A detailed analysis of the BCR signaling pathways revealed that the consequence of SYK inhibition on PLC γ 2 and AKT, as opposed to ERK1/2, was responsible for cell-cycle arrest. Genetic knock-down of these key molecules decelerated the proliferation of lymphoma cells. In addition, BCR signaling can be blocked by PRT060318 in primary lymphoma cells. Together, these

findings provide insights into cellular pathways required for lymphoma cell growth and support the rationale for considering SYK inhibition as a potentially useful therapy for DLBCL. The results further suggest the possibility of using PLC γ 2 and AKT as biomarkers to predict therapeutic response in prospective clinical trials of specific SYK inhibitors. (*Blood*. 2011;118(24):6342-6352)

Introduction

Diffuse large B-cell lymphoma (DLBCL) is one of the most common types of aggressive B-cell non-Hodgkin lymphomas. Pathologically, the tumor has a fast growth rate with a high Ki67 index. Without treatment, patients usually die within 6-24 months, and with current immunochemotherapeutic regimens, 50%-60% of patients can be cured. However, 40%-50% of patients remain refractory to the therapy. New agents are needed to improve survival.

Recently, BCR signaling has been recognized as a key pathway in the pathogenesis of DLBCL.¹ Many small molecules are under development to target the components of the pathway. Normal B cells are activated by Ag ligation of 2 Ig complexes on the B-cell surface that triggers BCR signaling.² In brief, the ligation activates the SRC family kinase that subsequently phosphorylates the ITAM motifs of Ig α and Ig β . Phosphorylated Ig α and Ig β recruit SYK kinase from cytoplasm to the perimembrane location to become associated with the BCR signalosome. SYK is then phosphorylated by SRC, auto-phosphorylated and activated, and subsequently interacts with and catalyzes the phosphorylation of several other signaling molecules, including PLC γ 2 (a lipase), BTK (a protein tyrosine kinase that also activates PLC γ 2), and BLNK (an adaptor molecule). Activated PLC γ 2 cleaves phosphatidylinositol 4,5-bisphosphate into diacylglycerol and inositol triphosphate, which leads to calcium mobilization and activation of several downstream pathways such as AKT, MAP kinase, and NF- κ B. Through these pathways, several transcriptional factors are activated and cells eventually undergo metabolic adaptation leading to increased cell survival, cell proliferation, differentiation into plasma or memory B cells, and Ab production.³

Several previous studies have shown that the BCR signaling plays a crucial role in the pathogenesis of DLBCL. By

gene-expression profiling and analysis of tumor cells in relation to normal B-cell subsets, Staudt et al identified a subtype of DLBCL (activated B cell-like DLBCL, also known as the ABC subtype) that carries a gene-expression signature resembling that of anti-IgM-activated peripheral blood B cells.⁴ Conversely, using gene-expression profiling and unsupervised consensus clustering for analysis, Shipp et al identified a subset of lymphoma that demonstrates a BCR/proliferation signature (BCR-type DLBCL). These lymphomas express high levels of SYK mRNA, along with other components of the BCR-signaling pathway.⁵ Previous studies from our group demonstrated that DLBCL have higher levels of tyrosine-phosphorylated proteins compared with the normal resting B cells. Using a pharmacologic approach, we also demonstrated that perturbation of BCR signaling with dasatinib, a SRC/LYN kinase inhibitor, blocks proliferation and BCR signaling in DLBCL cell lines and primary tissues that exhibit active BCR signaling.⁶ Most recently, using a shRNA functional screen, Staudt et al further demonstrated that chronic B-cell signaling is particularly active in the ABC type of DLBCLs that carry a wild-type *CARD11* gene.⁷ Decreasing the amount of BCR signal transducers such as IgM, Ig κ , Ig α , Ig β , BTK, and SYK was toxic to *CARD11* wild-type ABC cell lines. Moreover, somatic gain-of-function mutations in CD79B (Ig β) were identified in approximately 20% of primary ABC tumors.⁷

As a key component of the BCR signaling pathway,⁸ SYK represents a rational therapeutic target in DLBCL. Shipp et al have shown that DLBCL with the BCR signature is sensitive to R406, a drug that has activity against SYK.⁹ In a phase 2 clinical trial, fostamatinib, a pro-drug to R406, produced 4 partial

Submitted January 31, 2011; accepted October 5, 2011. Prepublished online as *Blood* First Edition paper, October 24, 2011; DOI 10.1182/blood-2011-02-333773.

The online version of this article contains a data supplement.

The publication costs of this article were defrayed in part by page charge payment. Therefore, and solely to indicate this fact, this article is hereby marked "advertisement" in accordance with 18 USC section 1734.

© 2011 by The American Society of Hematology

responses, 1 complete response, and 4 stable-disease responses among 23 relapsed/refractory DLBCL patients.¹⁰ However, these effects may or may not be a consequence of SYK inhibition because R406 inhibits other kinases in addition to SYK.^{11,12}

Despite these studies, it remains unknown whether SYK protein is expressed and activated in DLBCL tissues. It is also not clear whether selective SYK inhibition has a functional consequence on the cell cycle or on cell viability. In addition, the downstream signaling pathways that are important for the proliferation or survival of the malignant cells have not been well characterized. In the current study, we attempt to address these questions. Our detailed analysis of differential responses among lymphoma cells to SYK inhibition and SYK knock-down enabled a deeper understanding of the pathways leading to lymphoma proliferation. This information is important for future drug development efforts.

Methods

Cell lines, patient samples, and reagents

The human DLBCL cell lines OCI-LY1, OCI-LY4, OCI-LY7, OCI-LY8, OCI-LY18, Val, DHL-2, DHL-6, OCI-LY3, and OCI-LY10 were cultured in IMDM as described previously.⁶ For BCR stimulation, approximately $1-5 \times 10^6$ cells at log phase, treated or untreated with PRT060318, were incubated at 37°C for 15 minutes with a mixture of 5 µg/mL each of goat F(ab')₂ anti-human IgM and anti-human IgG (Southern Biotech). After washing with cold $1 \times$ PBS, the stimulated cells were harvested for subsequent analyses.

DLBCL tissues and frozen tumor cell suspensions were obtained from the tumor bank of the Department of Pathology at Weill Cornell Medical College and studied after Institutional Review Board review and approval. Thawed primary cells were cultivated in IMDM plus 20% FBS. The SYK inhibitor PRT060318 (PRT318) was provided by Portola Pharmaceuticals.

RNA preparation, reverse transcriptase, and quantitative PCR

Total RNA preparation, cDNA synthesis, and quantitative RT-PCR were performed as described previously.^{13,14} For details, see supplemental Methods (available on the *Blood* Web site; see the Supplemental Materials link at the top of the online article).

Immunoblotting assay

Immunoblotting was performed as described previously.^{13,15} The Abs used were purchased from the following sources: anti-SYK, anti-phospho-SYK (Tyr525/526), anti-PLCγ2, and anti-AKT were from Cell Signaling Technology; anti-β-actin was from Santa Cruz Biotechnology; and anti-GAPDH was from Thermo Fisher Scientific.

Tissue microarray construction and immunohistochemical staining

Tissue microarray was constructed as described previously.¹⁶ Immunohistochemical staining of phospho-SYK (Y525/526; rabbit polyclonal Ab; Cell Signaling Technology) was performed using the Bond Max Autostainer (Leica Microsystems). Formalin-fixed, paraffin-embedded tissue sections were deparaffinized and endogenous peroxidase was inactivated. Ag retrieval was accomplished using the Bond Epitope Retrieval Solution 1 (ER1) at 99-100°C for 30 minutes (Leica Microsystems). After retrieval, the sections were incubated sequentially with the primary Ab for 25 minutes, with the postprimary Ab for 15 minutes, and with the polymer for 25 minutes. Colorimetric development was accomplished by diaminobenzidine treatment for 10 minutes (Bond Polymer Refine Detection; Leica Microsystems). Finally, the sections were counterstained with hematoxylin, dehydrated, and mounted in Cytoseal XYL (Richard-Allan Scientific).

Specificity of PRT060318 (PRT318)

Kinomescan (Ambit Biosciences) service was used to determine the inhibitory activity of PRT318 against a panel of 318 purified kinases and their isoforms, as well as the binding constants of PRT318 for the selected panel of kinases.

Cell counting and metabolic activity

Cell growth was determined with live-cell counting by flow cytometry as described previously.⁶ Cell metabolic activity was measured with the MTT assay (Roche) following the manufacturer's instructions.

siRNA transfection

Pools of siRNA against human SYK and control scrambled siRNA (ON-TARGETplus SMARTpool) were purchased from Dharmacon RNAi Technologies/Thermo Scientific, and those against human PLCγ2 and AKT from QIAGEN. The siRNA targeting sequences are listed in supplemental Table 1. The DLBCL cells (10^5 cells/well, 1.5 mL/well) were seeded in 6-well plates and transfected with 1-4 µg of the specific siRNA or control scrambled siRNA pool using the X-tremeGENE siRNA transfection reagent (Roche Applied Science) or Lipofectamine LTX (Invitrogen) according to the manufacturer's instructions. For further details, see supplemental Methods.

Cell cycle and viability determination

The bromodeoxyuridine incorporation assay (BD Biosciences) was performed as described previously.⁶ The propidium iodide exclusion method⁶ or the PE annexin V Apoptosis Detection Kit I (BD Biosciences) was used to measure cell viability.

Immunofluorescence and confocal microscopy

To prepare cells for immunofluorescence and confocal microscopy, $1-5 \times 10^5$ DLBCL cells/mL were pretreated with various concentrations of PRT318 for 15 minutes, then stimulated with a mixture of 5 µg/mL of anti-IgM and 5 µg/mL of anti-IgG at 37°C for 15 minutes. Harvested cells were resuspended in 1-2 mL of ice-cold PBS and 2×10^4 cells were then placed in each well of a 24-well plate covered at the bottom with poly-L-lysine-coated glass coverslips (BioCoat; BD Biosciences). The plates were placed on ice for 15 minutes. Cells on the coverslips were then fixed with 4% paraformaldehyde and 1mM Na₃VO₄ in PBS for 15 minutes on ice. After the PBS wash, cells were permeabilized for 5 minutes at room temperature (RT) with 1% Triton X-100 in PBS, and incubated in blocking buffer (10% FCS, 0.1% Tween-20 in PBS) at RT for 1 hour. Permeabilized cells were then stained with a 1:800 dilution of anti-phospho-SYK (Tyr525/526) Ab (Cell Signaling Technology) for 4 hours to overnight. After 3 PBS washes, cells were incubated with a 1:2000 dilution of Alexa Fluor 488-conjugated goat anti-rabbit IgG Ab (Invitrogen) at RT for 2 hours.

For staining of cell-surface IgM (LY7 and LY18) or IgG (LY3), cells on the coverslips were stained with either a 1:1000 dilution of anti-IgM or anti-IgG (Invitrogen). After washing, cells were incubated with Alexa Fluor 594-conjugated goat anti-mouse IgG Ab (Invitrogen) at RT for 2 hours. After staining and PBS washing, the coverslips were mounted onto glass slides and sealed. Slides were then subjected to confocal microscopy examination using the Leica TCSSP5 system, and images were acquired using MetaMorph 7.7 software (Molecular Devices).

Phosphoflow analyses

Phosphoflow analyses of DLBCL cells were performed as described previously.^{6,17} For further details, see supplemental Methods.

Statistical analyses

Statistical analyses and IC₅₀ determination were performed using Prism 5.1 software (GraphPad). The relationship between SYK mRNA gene expression and SYK protein levels was analyzed by linear regression and Pearson correlation.

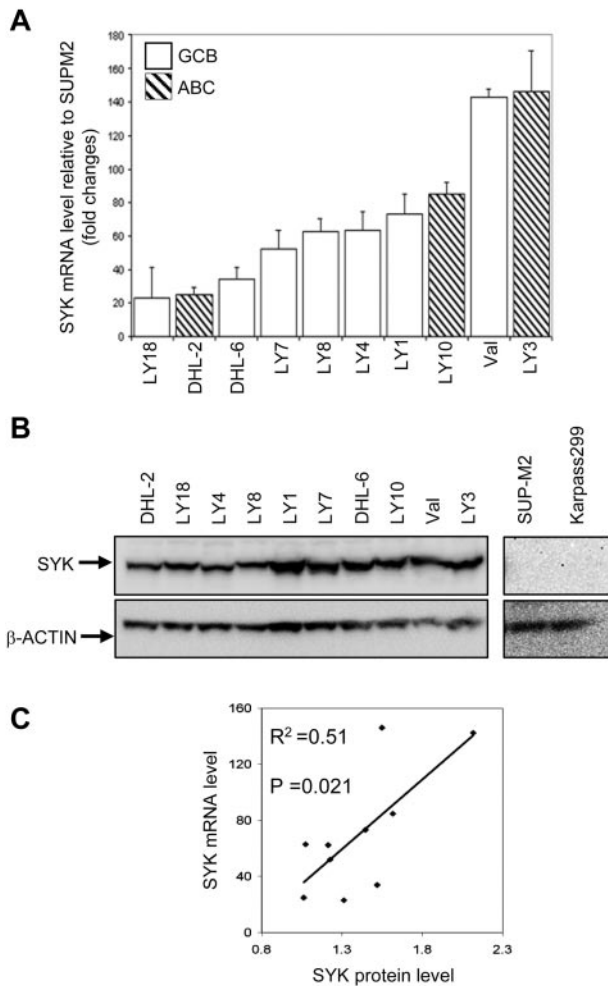


Figure 1. SYK is expressed in a panel of DLBCL cell lines. (A) Expression of SYK mRNA in a panel of 10 GCB-type or ABC-type DLBCL cell lines by real-time PCR. PKG1 was used as the internal control gene for normalization. Results were expressed as relative expression to SUP-M2, a T-cell lymphoma cell line that does not express a significant amount of SYK. Error bars show means \pm SD from 3 independent experiments with duplicate reactions. (B) Expression of SYK protein in the cell lines by immunoblotting. β -actin was included as a loading control. (C) Correlation between SYK mRNA and protein levels was analyzed by linear regression. The level of significance was set at $P = .05$.

Results

Quantification of SYK expression in a panel of DLBCL cell lines

We first screened for SYK expression in a panel of DLBCL cell lines at both the mRNA and the protein level. The cell lines include 7 GCB cell lines: OCI-LY1 (LY1), OCI-LY4 (LY4), OCI-LY7 (LY7), OCI-LY8 (LY8), OCI-LY18 (LY18), SU-DHL-6 (DHL6), and VAL, as well as 3 ABC cell lines: OCI-LY3 (LY3), OCI-LY10 (LY10), and SU-DHL-2 (DHL2). The level of SYK mRNA expression was determined by quantitative RT-PCR (Figure 1A). Compared with SUP-M2, a T-cell lymphoma line, DLBCL had a 20- to 150-fold increase in SYK mRNA expression. SYK proteins were also expressed at elevated levels in DLBCL relative to both SUP-M2 and Karpas 299, another T-cell lymphoma cell line (Figure 1B). Logistical regression analysis revealed only a weak correlation between SYK mRNA and protein expression in the lymphoma cell lines (Figure 1C), suggesting that posttranscriptional regulation may play a role in the control of SYK protein expression. There

was no apparent correlation between the levels of SYK in the GCB versus ABC subtypes of DLBCL.

SYK is activated in primary lymphoma tissues

Although it has been shown that SYK mRNA is expressed in DLBCL,⁵ the amount, cellular localization, and activation status of SYK protein has never been evaluated in DLBCL tumor tissues. To determine whether SYK is relevant in the pathogenesis of DLBCL, we developed an immunohistochemical staining assay for p-SYK (pY525/526) expression on a tissue microarray of DLBCL tumors. Phosphorylation of SYK at tyrosine 525/526 represents the active form of SYK because these residues are auto-phosphorylated by SYK itself after BCR stimulation and SRC activation.

To establish the assay, we first tested whether LY7 and LY18 cells could serve well as controls. We demonstrated by immunoblotting that, although total SYK was present in both stimulated and unstimulated lymphoma cells (\pm anti-BCR), SYK was phosphorylated only when LY7 and LY8 cells were stimulated (Figure 2A). Cell blocks of unstimulated and stimulated LY7 cells were then made and stained with anti-pY525/526. Figure 2B showed that upon BCR ligation with Abs, the intensity of p-SYK staining increased dramatically, which is consistent with the immunoblotting data (Figure 2A). In addition, the staining showed a characteristic circular membrane pattern that is consistent with the fact that SYK is recruited from the cytoplasm to the perimembrane location to become part of the BCR signalosome upon stimulation (Figure 2B). Stimulated LY18 cells also demonstrate membrane staining of p-SYK, confirming the findings in LY7 cells. The immunoblotting and cell block results indicate that the staining was specific for active SYK at the right subcellular locations under the right conditions.

With these controls, we applied the immunohistochemical staining procedure to a large array of DLBCL primary tissues and normal lymphoid tissues. Normal tissues, including tonsil, appendix, thymus, and spleen (with extramedullary hematopoiesis), stained negative for p-SYK (Figure 2C), whereas many DLBCL tissues exhibited p-SYK expression with a characteristic membrane staining (Figure 2D). Of 61 evaluable DLBCL tumor tissues, a total of 27 (44%) stained positive for p-SYK; 18 of 27 were scored 1+, 4 were scored 2+, and 5 were scored 3+. These tumor tissues were subclassified into GCB and non-GCB phenotypes using the Hans immunohistochemical staining method,¹⁸ which is approximately 80% concordant with the gene-expression profiling classification of GCB and ABC subtypes.¹⁹ Of these 27 lymphomas with the active form of SYK, 15 belonged to the non-GCB type and 10 belong to the GCB type. These results demonstrate for the first time that SYK kinase is phosphorylated and is located primarily in the membranes of DLBCL cells. Therefore, SYK kinase is active in a significant number of DLBCL tumors regardless of their subtypes.

DLBCL cells are inhibited by a specific SYK inhibitor with different sensitivities

To determine whether SYK is functionally important in DLBCL, we investigated whether specific inhibition of SYK kinase activity has any effects in DLBCL cell lines. We first used PRT060318 (abbreviated as PRT318 hereafter), a specific SYK inhibitor. When tested against a large panel of 318 purified kinases in a biochemical assay, this compound reduced the activity of SYK and 10 other kinases by 60%-100% at 300nM, a concentration that is 75-fold above its SYK IC_{50} of 4nM²⁰ (Table 1). Most of the unintended kinases that PRT318 did inhibit at this concentration are not significantly expressed in primary lymphoma tissues (www.proteinatlas.org). The binding constants of PRT318 for these kinases are

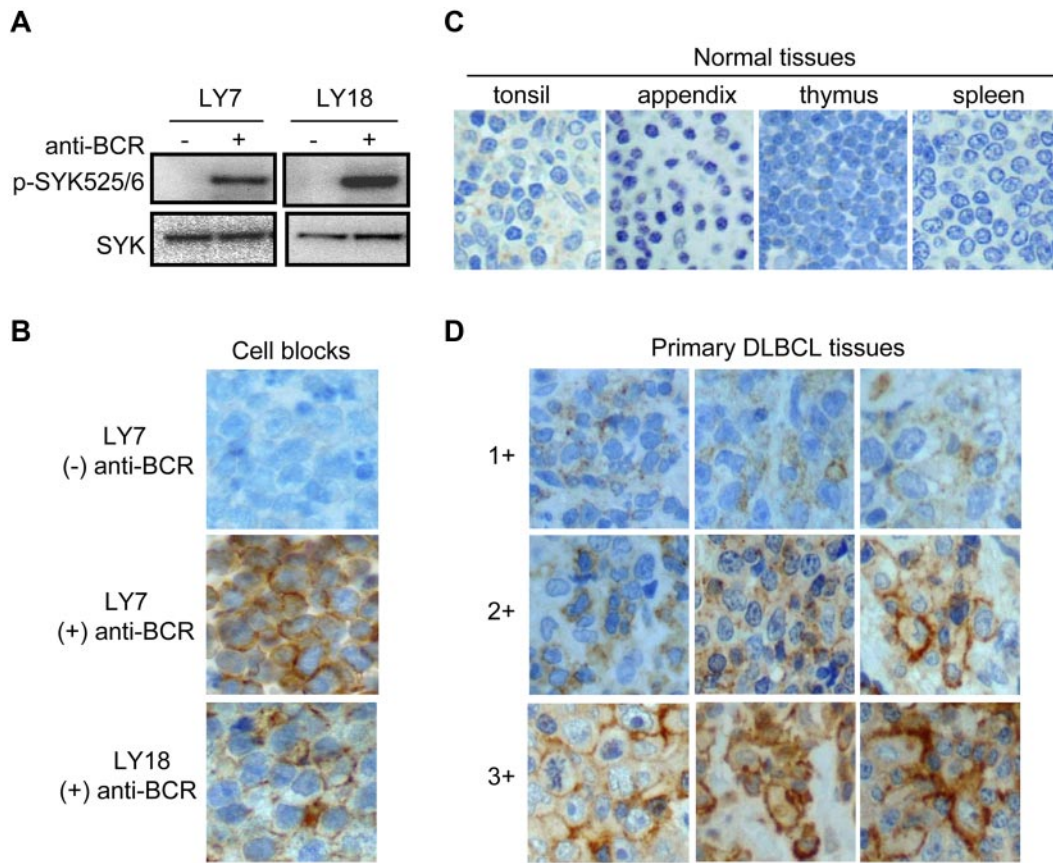


Figure 2. SYK is activated in primary DLBCL tissues. (A) Immunoblotting of total and phosphorylated SYK (pY525/526) in LY7 and LY18 cell lines. Cells were stimulated with (+) or without (-) anti-BCR as described in "Methods." (B) Immunohistochemical staining of p-SYK (pY525/526) on sections of paraffin cell blocks made from anti-BCR stimulated (+) or unstimulated (-) LY7 and LY18 cells. Photomicrographs were generated using Nikon E600, Planachromat 4/0.10/30.0, 20/0.40/1.3, PlanApo 40/0.095/0.12-0.16, and PlanFluor 40/0.75/0.72 objectives, and were captured using an Olympus DP12 camera. (C-D) Immunohistochemical staining of p-SYK on paraffin-embedded sections from tissue microarray in normal lymphoid tissues (C) and DLBCL tissues (D). The ranges for the scoring system are shown.

shown in supplemental Table 2. The drug did not inhibit the remaining approximately 300 kinases and their isoforms at 300nM (supplemental Table 3). These analyses demonstrated PRT318 to be a highly selective and potent SYK inhibitor. The selectivity of the drug for SYK was also demonstrated with an independent assay in a recent report on the efficacy of PRT318 in heparin-induced thrombocytopenia.²⁰

The effects of PRT318 on 10 DLBCL cell lines were determined using a cell-based MTT assay at a wide range of concentrations

(Figure 3A). Among these cell lines, LY1, LY7, LY8, LY10, LY18, VAL, and DHL-6 had IC₅₀ values below 3.5 μM (Figure 3B); LY3, LY4, and DHL-2 had IC₅₀ values at or above 14 μM. Because there was a clear demarcation between these 2 groups with regard to IC₅₀, we defined them as sensitive and resistant cell lines, respectively. Higher concentrations required for cellular assays compared with biochemical assays are expected and similar observations have been reported previously.²¹ Based on the differential sensitivities among the DLBCL cell lines, all subsequent experiments were conducted at concentrations of 3 μM or below.

We subsequently analyzed the effects of PRT318 on cell proliferation. The numbers of cells treated with various doses of PRT318 were followed over time. Figure 3C shows that the growth of sensitive LY7 and LY18 cells was inhibited by the inhibitor in a dose-dependent fashion. In contrast, such dose-dependent inhibition was not apparent with the resistant LY3 and LY4 cells.

Table 1. Kinases inhibited by PRT318 and their expression in tissues

Kinase	Inhibition, %*	Expression in normal lymph nodes†	Expression in primary lymphoma tissues†
PAK4	99.8	Moderate	Mostly Negative
PAK7	99.2	Negative	Negative
PAK6	91.6	Negative	Negative
SYK	91.6	Strong	Strong
ANKK1	91.4	Weak	Weak To Moderate
MAP3K9	82	Negative	Negative
DAPK1	80	ND	ND
EIF2AK2	77	Strong	Mostly Negative
MYLK4	72	Weak	Negative
STK33	68	Strong	Mostly Strong
PHKG2	60	ND	ND

ND indicates no data.

*Percent inhibition of kinase activity tested against 300nM PRT318.

†Tissue microarray data were retrieved from a proteomics website (www.proteinatlas.org).

Growth of sensitive DLBCL cells is inhibited by siRNA against SYK

To further demonstrate that the cell proliferation effect was caused by the specific inhibition of SYK, we used RNA interference to specifically target SYK. Sensitive LY18, LY7, as well as resistant LY4 cells were transfected with either a pool of siRNA against SYK or a pool of scrambled siRNA. Figure 4A shows that the level of SYK protein was significantly reduced in cells transfected with SYK siRNA compared with those transfected with scrambled siRNA. Cell proliferation was also followed in transfected cells

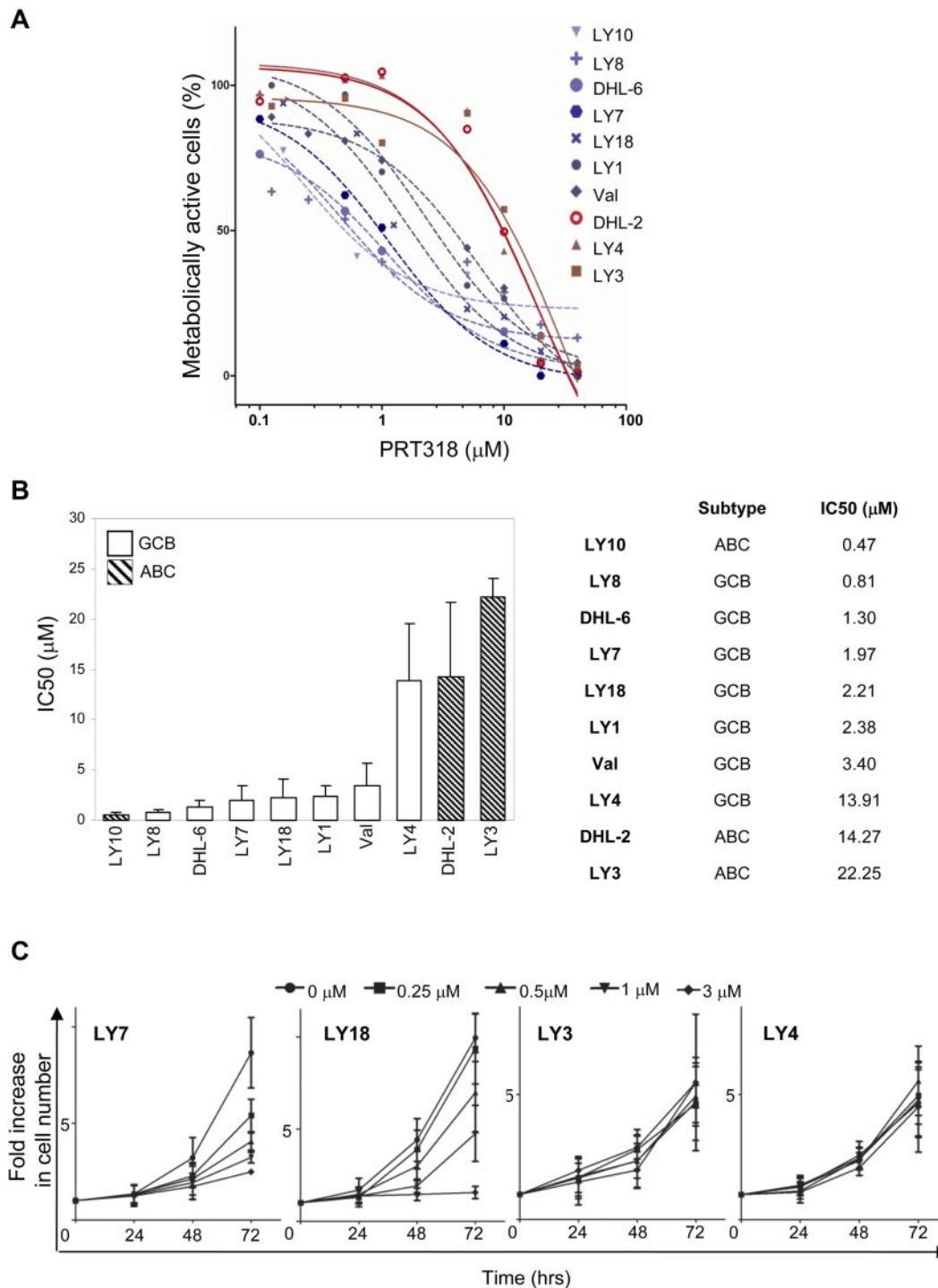


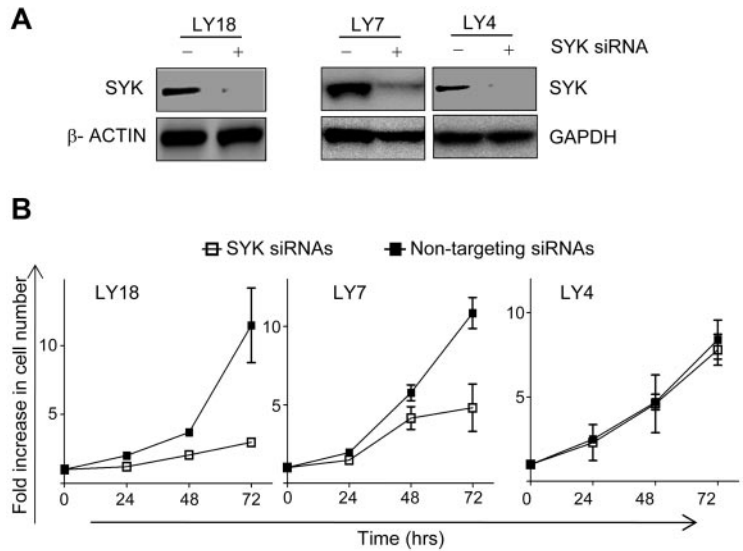
Figure 3. DLBCL cells are inhibited by a specific SYK inhibitor with different sensitivities. (A) The IC_{50} values of PRT318 for DLBCL cell lines were determined using the MTT assay over a wide range of concentrations. (B) Bar graphs and tables showing precise values of IC_{50} for the cell lines. Error bars show means \pm SD of results from 3 independent experiments. (C) PRT318 inhibits growth of the sensitive cell lines in a dose-dependent manner. Two sensitive (LY7 and LY18) and 2 resistant (LY3 and LY4) cell lines were treated with indicated doses of PRT318. The -fold increase in cell number indicates viable cell number at the indicated time point relative to time 0.

(Figure 4B). Whereas scrambled siRNA-transfected cells continued to double, the proliferation of SYK siRNA-transfected cells was inhibited in LY18 and LY7 cells. In resistant LY4 cells, doubling was not significantly affected by the SYK knockdown. These results show that genetic reduction of SYK phenocopied the effects of SYK kinase inhibition. These results confirm that SYK plays an important role in the proliferation of DLBCL cells.

Inhibition and genetic knock-down of SYK cause cell-cycle arrest in sensitive DLBCL cells

To determine what specific cellular effects are caused by SYK inhibition, we analyzed cell-cycle progression and apoptosis of DLBCL lines in the presence or absence of PRT318. Using bromodeoxyuridine and 7-amino-actinomycin D (7-AAD) double staining, the effects of PRT318 on different phases of the cell cycle

Figure 4. Growth of sensitive DLBCL cells is inhibited by siRNA against SYK. (A) Immunoblots of SYK protein in LY18, LY7, and LY4 cells that were transfected with a scrambled (-) or a SYK-specific (+) siRNA pool. β -actin or GAPDH was blotted as a loading control. (B) Simultaneous cell counting was conducted at the indicated times after transfection. The -fold increase in cell number indicates viable cell number relative to those at time 0.



were determined. As shown in Figure 5A, in the LY7 and LY18 cell lines, the fraction of cells in the S phase was significantly reduced by 48-hour treatment of cells with increasing doses of PRT318 (Figure 5A top 2 rows). This change was accompanied by a concomitant increase in the number of G₀/G₁ cells. Conversely, this effect by the inhibitor was not observed in the resistant LY3 and LY4 cell lines (Figure 5A bottom 2 rows). These results suggest that SYK inhibition results in cell-cycle arrest at the G₀/G₁ phase.

We then assessed cell viability using annexin V and 7-AAD double staining in cells treated with increasing doses of PRT318 (Figure 5B). Nearly 90% of LY7 and LY18 cells remained alive after a 96-hour treatment with 3 μ M PRT318. These data demonstrate that the primary effect of SYK inhibition is on the cell cycle and not on cell viability.

Knockdown of SYK decelerated cell growth (Figure 4A), so we analyzed whether this change in cellular phenotype by SYK

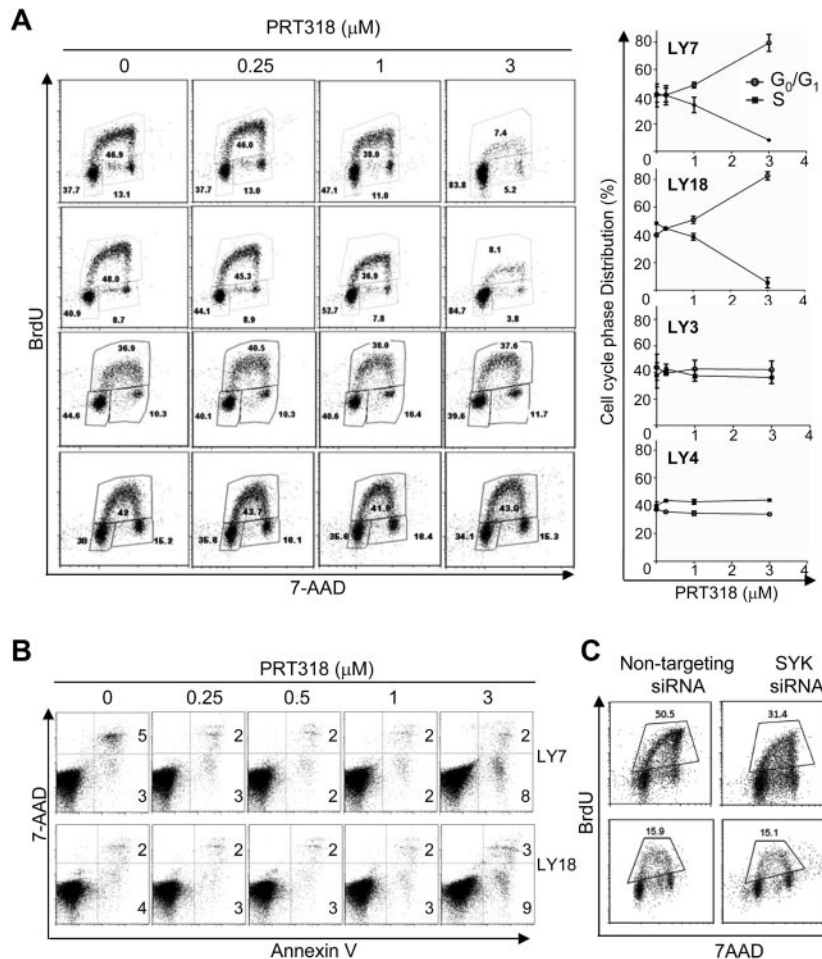


Figure 5. SYK inhibition causes cell-cycle arrest only in sensitive DLBCL cells. (A) Effects of PRT318 on cell proliferation were measured by 7-AAD/bromodeoxyuridine (BrdU) incorporation. Two sensitive (LY7 and LY18) and 2 resistant (LY3 and LY4) cell lines were treated for 48 hours with various concentrations of PRT318, as indicated at the top of the dot plots. Percentages of events in each gate were indicated in each of the plots. Quantification of S and G₀/G₁ phase events are shown in the line graphs next to the dot plots. (B) Effects of PRT318 on cell viability were measured by annexin V/7-AAD double staining. The cell lines were treated for 96 hours with various concentrations of PRT318, as indicated at the top of the dot plots. Percentages of events in each quadrant were indicated in each of the plots. (C) Effects of SYK siRNA on cell proliferation. LY18 and LY4 were transfected with SYK or control siRNA pools and cell proliferation was measured by 7-AAD/BrdU incorporation at 48 hours after transfection.

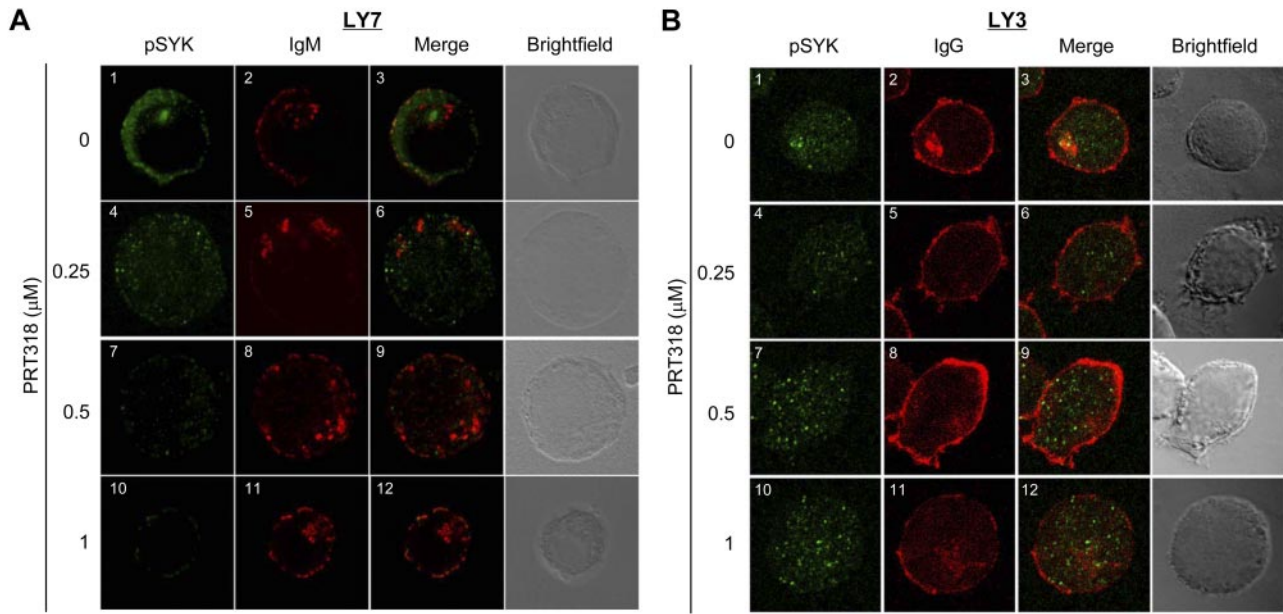


Figure 6. Effects of PRT318 on SYK phosphorylation in sensitive and resistant DLBCL cells. (A) Confocal images of sensitive LY7 cells treated with or without various concentrations of PRT318 as indicated on the left of the images. Proteins labeled are indicated at the top of the images. Merged and bright-field images are also shown. (B) Confocal images of resistant LY3 cells treated with or without various concentrations of PRT318, as indicated on the left of the images. Molecules labeled are indicated on top of the images. Merged and bright-field images are also shown.

siRNA, like that caused by PRT318, was a result of a decrease in cycling cells. As shown in Figure 5C, SYK-targeting siRNA reduced the S-phase events in sensitive LY18 cells but not in resistant LY4 cells. These data provided additional evidence that SYK is required for lymphoma cell proliferation.

Effects of PRT318 on SYK phosphorylation in sensitive and resistant DLBCL cells

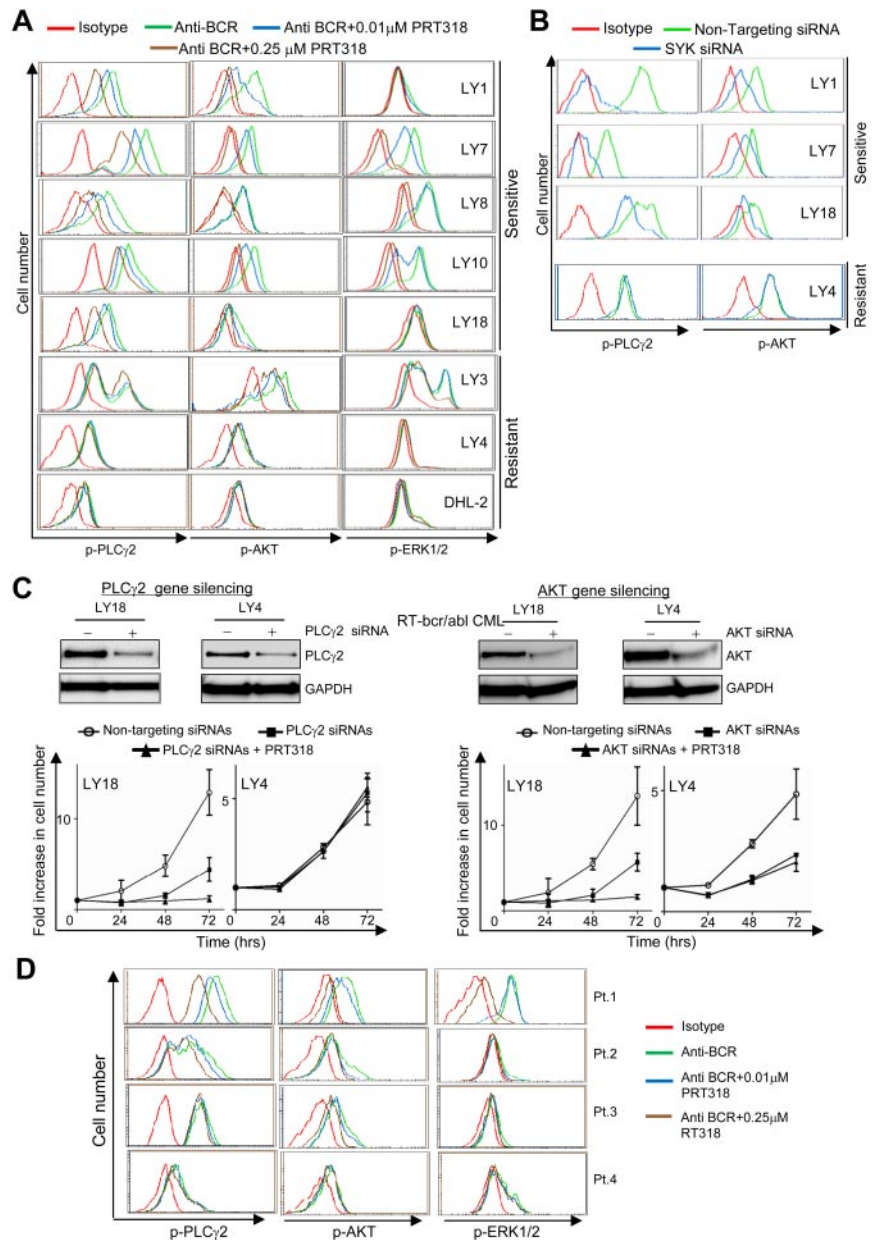
To further understand the molecular basis that determines the response to SYK inhibition, we examined the subcellular location and intensity of p-SYK in PRT318-treated and untreated cells using confocal microscopy. As shown in Figure 6A1, p-SYK (green) was accumulated at the perimembrane location in untreated LY7 cells after BCR stimulation. This pattern is similar to what we observed previously using the immunohistochemical technique (Figure 2B). IgM is the major IgH on the surface of LY7 cells (supplemental Figure 1). Staining of membrane IgM (red dots in Figure 6A2) revealed that some of the p-SYK molecules are colocalized in the BCR microclusters on the cell membrane (yellow dots on the cell surface in Figure 6A3). Increasing the concentration of PRT318 from 0.25 to 1 μ M not only reduced the intensity of p-SYK, but the location of p-SYK was also changed from a perimembrane site to a cytoplasmic distribution (Figure 6A4, 6A7, and 6A10). Conversely, the intensity and distribution of IgM were not significantly affected (Figure 6A5, 6A8, and 6A11 and 6A6, 6A9, and 6A12, respectively). Similar observations were made in LY18 cells, another sensitive cell line (supplemental Figure 2). The same experiment was performed on the resistant LY3 cells that were stimulated with Ab against IgG, the major form of the heavy chain on the cell surface (supplemental Figure 1). In contrast to LY7 cells, p-SYK was distributed in the cytoplasm and did not respond to BCR stimulation (Figure 6B1). Further, p-SYK in LY3 cells was not significantly affected by the presence or absence of the SYK inhibitor (Figure 6B4, 6B7, 6B10, and the remaining panels).

Dose-dependent inhibition of BCR signaling in sensitive but not resistant DLBCL cells: PLC γ 2 and AKT mediate the effects of SYK on cell proliferation

We next examined whether there are any differential uses of downstream pathways in responsive versus resistant DLBCL cells. After BCR ligation and SYK phosphorylation, several pathways were activated, including (1) PLC γ 2 phosphorylation leading to PKC and NF- κ B activation, (2) PI3K activation leading to AKT phosphorylation, and (3) RAS-RAF activation leading to the activation of MAPK and ERK phosphorylation. For a detailed and precise comparison of phosphorylation of PLC γ 2, AKT, and ERK between sensitive (LY1, LY7, LY8, LY10, and LY18) and resistant (LY3, LY4, and DHL2) cell lines, we applied intracellular phospho-specific flow cytometric analysis, a highly sensitive and quantitative assay. The cell lines were pretreated with vehicle or different doses of PRT318, followed by BCR stimulation with anti-IgM/anti-IgG or isotype control. The cells were then simultaneously stained and analyzed for phosphorylation of PLC γ 2, AKT, and ERK1/2. As shown in the left column of Figure 7A, BCR stimulation in the sensitive cell lines LY1, LY7, LY8, LY10, and LY18 caused a marked increase in the phosphorylation of PLC γ 2: compare the green traces with red traces. Increasing concentrations of PRT318 resulted in a concentration-dependent decrease in p-PLC γ 2: compare 0 μ M (green), 0.01 μ M (blue), and then 0.25 μ M (brown) traces. In contrast to the sensitive cell lines, the 3 resistant cell lines (LY3, LY4, and DHL2) did not demonstrate significant left shifts with the drug treatment. For AKT phosphorylation (Figure 7A middle column), dose-dependent left shifts were evident in all 5 sensitive cell lines and were minimal in the 3 resistant cell lines. For p-ERK1/2, mixed results were obtained (Figure 7A right column). In cell lines in which BCR stimulation caused significant increase in p-ERK (LY3, LY7, LY8, and LY10), decrease in p-ERK occurred with inhibitor treatment and was unrelated to sensitivity of the cell lines to the anti-proliferative

Figure 7. Molecular mechanisms that determine responses of DLBCL to SYK inhibition or reduction.

(A) Dose-dependent inhibition of BCR signaling in sensitive but not resistant DLBCL cell lines. Simultaneous phospho-flow analyses of p-PLC γ 2 (left column), p-AKT (middle column), and p-ERK1/2 (right column) in DLBCL cell lines indicated on the right. Red traces indicate isotype control; green, cells stimulated with anti-BCR in the absence of PRT318; blue, stimulated cells treated with a 0.01 μ M concentration of inhibitor; and brown, stimulated cells treated with a 0.25 μ M concentration of drug. (B) Effects of SYK siRNA on PLC γ 2 and AKT phosphorylation. LY1, LY7, LY18, and LY4 were transfected with SYK (blue traces) or control (green) siRNA pools. Phosphorylation was measured by the phospho-flow assays 48 hours after transfection. (C) Top panels show immunoblots of PLC γ 2 or AKT protein in LY18 and LY4 cells transfected with PLC γ 2 (+), AKT (+), or control siRNA (-) pools. GAPDH was blotted as a loading control. Bottom panels show simultaneous cell counting conducted at the indicated times after transfection. The fold increase in cell number indicates viable cell numbers relative to those at time 0. (D) Inhibition of BCR signaling in primary DLBCL lymphoma cells. Simultaneous phospho-flow analyses of p-PLC γ 2 (left column), p-AKT (middle column), and p-ERK1/2 (right column) in primary DLBCL tumor cells. Color legends are as in panel A. Pt indicates patient.



effects of PRT318. In those cell lines in which BCR stimulation did not induce ERK phosphorylation (LY1, LY4, LY18, and DHL2), PRT318 treatment had no effect. Therefore, changes in p-ERK are not related to the cellular proliferative response of these cell lines.

We then tested whether siRNA knockdown of SYK would generate the same effect on PLC γ 2 and AKT phosphorylation as the pharmacologic intervention with PRT318. Figure 7B shows that p-PLC γ 2 and p-AKT were reduced by SYK siRNA (blue) compared with scrambled control (green) in sensitive LY1, LY7, and LY18 cells, but not in resistant LY4 cells.

To further investigate whether PLC γ 2 and AKT mediate the effects of SYK on cell proliferation, we investigated whether, like SYK knockdown, direct knockdown of the molecules would also affect cell growth. Figure 7C shows that the siRNA effectively reduced the amount of PLC γ 2 protein (Figure 7C top left) and decreased significantly the rate of cell proliferation in sensitive LY18 cells, but not in resistant LY4 cells (Figure 7C

bottom left panel). In addition, treatment of siRNA-transfected cells with PRT-318 further suppressed the growth of LY18 but not LY4 cells. This added effect in LY18 was expected because siRNA reduced, but did not completely eliminate, the PLC γ 2 protein (Figure 7C Western blots).

Interestingly, AKT siRNA decelerated the growth of PRT318-sensitive LY18 cells and resistant LY4 cells (right panel). Treating AKT siRNA-transfected cells with PRT318 further blocked LY18 growth but did not affect LY4 growth. LY4 only responded to AKT reduction, not SYK inhibition or reduction. These results suggest that: (1) A complete shut-down of the SYK-PLC γ 2-AKT pathway is required to stop cell growth in sensitive LY18 cells and (2) a SYK-independent downstream event that activates AKT drives proliferation in resistant LY4 cells.

Together with the confocal results, our data demonstrate that the activities of SYK, PLC γ 2, and AKT determine the cellular responses to SYK inhibition. From a pathogenic perspective,

these results suggest that sensitive cells rely on the pathways via SYK-PLC γ 2-AKT, but not ERK1/2, for proliferation.

Inhibition of BCR signaling in primary DLBCL lymphoma cells

To determine whether BCR signaling can be inhibited in primary DLBCL cells from patients, we treated several specimens of freeze-thawed lymphoma cells with different concentrations of PRT318 and performed phospho-flow assays. Each sample contained > 80% lymphoma cells as assessed by flow cytometry. Similar to cell lines, patient lymphoma cells responded to anti-BCR stimulation (compare red and green traces in Figure 7D). In terms of p-PLC γ 2 and p-AKT, the activated BCR signaling showed a dose-dependent suppression by the drug in some patients (Figure 7D patients 1 and 2), but little response in others (Figure 7D patients 3 and 4). Because the thawed lymphoma cells do not proliferate and die quickly in vitro, the functional consequences of these differences among the patients could not be assessed. Despite that, these results demonstrate the phospho-flow technique can be applied to preserved primary cells, and therefore these assays have the potential to serve as biomarkers for response prediction in patients. Our results also demonstrate that BCR signaling pathways can be blocked by a highly specific SYK inhibitor in a subset of primary lymphoma cells.

Discussion

The present study contributes several pieces of previously unknown information regarding role of SYK in the pathogenesis of DLBCL. First, the expression levels, subcellular localization, and activation status of SYK protein in DLBCL have never been studied before. Using a tissue microarray, we demonstrate herein that the SYK protein is phosphorylated, localized to the cell membrane, and therefore activated in 44% of human DLBCL tissues. We have also pinpointed the specific cellular effect caused by SYK inhibition: cell-cycle arrest. This knowledge may inform rational drug combination in the treatment of DLBCL in both preclinical and clinical settings. Our results also show that PLC γ 2 and AKT, as opposed to ERK, connect SYK to cellular proliferative responses. PLC γ 2 and AKT phosphorylation responded to SYK inhibition and reduction in a delicate, dose-dependent fashion in sensitive but not resistant cell lines. Moreover, knockdown of either PLC γ 2 or AKT decelerated cell growth. These results suggest that these 2 molecules relay signals from BCR/SYK to cause excessive cell proliferation in sensitive lymphoma cells. ERK was not required for this process, which is in agreement with a previous finding in SYK-deficient mice that activation of the Ras and MAPK pathway can be independent of SYK.²² We have also shown that the phospho-flow assays can be applied to freeze-thawed primary lymphoma specimens that demonstrated differential signaling responses to the SYK inhibitor. Together with the data on cell line sensitivities, the profiles of PLC γ 2 and AKT showed promise as in vitro biomarkers to predict clinical responses of DLBCL to SYK inhibition. However, the predictive capacity of these markers in a given lymphoma will need to be tested in a prospective clinical study that determines the protein phosphorylation profiles before patient clinical outcome. Our work made it feasible to test such a hypothesis in future clinical trials of specific SYK inhibitors. Finally, our studies used a novel and highly specific SYK inhibitor (Table 1 and supplemental Table 1) at low concentrations to ensure that the effects we observed were the result of the specific inhibition of SYK. In addition, genetic

knockdown of SYK was used to consolidate our conclusions drawn from these findings.

PRT318 is highly specific against SYK kinase (Table 1 and supplemental Tables 2 and 3). At a concentration of 0.3 μ M, 75 times higher than the IC₅₀ for SYK, PRT318 did not inhibit approximately 300 kinases, including ERK1/2, in the biochemical screening (Table 1 and supplemental Table 3). However, it appeared that p-ERK was inhibited by 0.25 μ M PRT318 in a small population of LY3 cells (Figure 7A line LY3, p-ERK, brown trace) despite the fact that p-SYK (Y525/526) was largely unaffected by PRT318 in the confocal study (Figure 6B). A possible explanation for this apparent discrepancy may lie in the sensitivities of these 2 different assays. In a small subset of LY3 cells, p-PLC γ 2, an immediate downstream target of SYK, was inhibited by PRT318 at a 0.25 μ M concentration by the highly sensitive and quantitative phospho-flow assay (Figure 7A line LY3, p-PLC γ 2, brown trace). These results suggest that SYK may be affected in the small LY3 subset that was not detected by the confocal examination. p-ERK inhibition may therefore be explained as a subsequent effect of PRT318 inhibition of SYK in a minority of LY3 cells.

The concept of SYK inhibition in DLBCL was explored previously by Shipp et al using R406.⁹ However, it has become clear that R406 lacks selectivity for SYK.^{11,12} Our combination of pharmacologic and genetic approaches allows us to reach a more definitive conclusion that SYK is required for the proliferation of lymphoma cells. In the future, treating DLBCL with specific SYK inhibitors without affecting additional kinases may reduce toxicological consequences in patients.

Overall, our data did not find a strict correlation between the responses to SYK inhibition and lymphoma cell-of-origin subtypes: sensitive or resistant cell lines could be of either the GCB or ABC type, and for primary tumors, subtype information was available for patients 2 and 3, both of whom had GCB-type tumors. However, patient 2's lymphoma responded to the drug in vitro whereas patient 3's did not (Figure 7D). In addition, the presence or absence of SYK phosphorylation was not correlated with GCB or non-GCB subtypes by immunohistochemistry (Figure 2). These findings were unexpected after a recent publication by Staudt et al⁷ showing that approximately 30% of ABC-type DLBCL patients had genetic evidence of chronically active BCR signaling, in contrast to only a few percent of GCB-type DLBCL patients. Their data also showed that the ABC-type cell lines responded better to SYK knock-down than the GCB type. Among the ABC cell lines, LY3 was indeed resistant to SYK shRNA, which is consistent with our pharmacologic findings (potential mechanisms discussed in the paragraph below). Unfortunately, most of the GCB and ABC cell lines used in our study were not examined in that previous work, making direct comparison difficult.

Comparing the findings of Shipp et al⁹ and ours, among 7 cell lines that were commonly studied, sensitivity profiles to PRT318 in our study largely agree with those to R406 in Shipp et al. Specifically, both groups found that the cell lines LY1, LY7, LY10, LY18, and DHL-6 were sensitive and LY4 was resistant to SYK inhibition. The only disagreement between these 2 studies of these 7 lines was LY3, which was sensitive to R406 and resistant to PRT318. LY3 does not depend on SYK activity because it carries downstream activating mutations in *CARD11* and *MYD88*.²³ Its sensitivity to R406 may be explained by the activity of R406 toward other kinases in addition to SYK.^{11,12} Because consensus clustering has identified LY1, LY7, LY10, LY18, DHL-6, and LY3 as the BCR type,⁹ the 2 studies together indicate that active BCR

signaling is the key determinant of DLBCL responsiveness to SYK blockade.

The sensitivity of some GCB-type DLBCLs to SYK inhibition is not totally unexpected in view of other published data on the relationships among GCB-like DLBCL, SYK, and BCL-6. BCL6, a transcriptional repressor, is highly expressed in the germinal center and is used clinically as an immunophenotypic marker for GCB-type DLBCL in particular.¹⁸ It has been shown that, functionally, BCL6 indirectly up-regulates SYK activity by repressing PTPROt, a protein tyrosine phosphatase that inactivates SYK.²⁴ Therefore, BCL6-expressing GCB tumors may have increased SYK activity that makes them vulnerable to SYK inhibition. In support of this, most DLBCL tumors that are sensitive to BCL6 inhibition carry the BCR signature (including SYK).^{25,26} Although further studies are required, previous results together with our current findings raise the possibility that some GCB cell lines/tumors may functionally rely on BCR signaling.

Analysis of the cell line data revealed a variety of mechanisms that may be responsible for cellular resistance to SYK inhibition. (1) The lack of surface IgH contributes to nonresponse; DHL-2 cells had no detectable IgM or IgG either in cytoplasm or on the cell surface (supplemental Figure 1), whereas LY4 had only cytoplasmic IgM. (2) Defects in SYK recruitment from the cytoplasmic location to the perimembrane location is another factor that contributes to nonresponse to SYK inhibition. This is evident in LY3, which indeed has surface IgG, but SYK in LY3 failed to respond to the anti-IgG stimulation with subcellular translocation (Figure 6B). (3) Components downstream of SYK may also become constitutively active, resulting in SYK-independent cell growth. In fact, recent work by Staudt et al detected mutations in *CARD11*, a downstream molecule, in LY3 cells.²³ Most recently, *MYD88* mutations that lead to the activation of JAK/STAT signaling were discovered in both LY3 and DHL-2 cells, providing additional explanations as to why these cells do not respond well to SYK inhibition.²⁷ (4) In LY4, our own data suggest the existence of SYK-independent AKT activation (Figure 7C). Because the defects leading to resistance vary among cell lines and are largely SYK

independent, measurements of levels of SYK or p-SYK are irrelevant with regard to response prediction. The effects of the drug on the phosphorylation of PLC γ 2 and AKT are more reliable as response predictors, as demonstrated by our present data.

In conclusion, the results of our study not only show that SYK holds promise as a therapeutic target for DLBCL, but also identify potential biomarkers for therapeutic response prediction that can be used for future clinical trials of SYK inhibitors. From the perspective of pathogenesis, our results show that the PLC γ 2 and AKT pathways are particularly important for the proliferation of DLBCL, thus providing foci for future drug development efforts.

Acknowledgments

The authors thank Yifang Liu, Sharon Baroak, and Robert Kim for their assistance with immunohistochemical analysis of SYK.

Authorship

Contribution: S.C. and G.C. developed the assays, designed and performed the experiments, solved technical problems, analyzed the data, and wrote part of the manuscript; X.H.Z., R.S., Z.S., and P.L. performed the experiments and analyzed the data; A.M.M. contributed useful discussions and suggestions; A.P. and U.S. provided critical reagents and contributed useful suggestions; and Y.L.W. formed the hypothesis, directed and coordinated the project, designed the experiments, analyzed the data, and wrote the manuscript.

Conflict-of-interest disclosure: G.C., A.P., and U.S. are employees of Portola Pharmaceuticals Inc, and the study was partially supported by research funding from Portola. The remaining authors declare no competing financial interests.

Correspondence: Y. Lynn Wang, MD, PhD, Department of Pathology and Laboratory Medicine, Weill Cornell Medical College, 1300 York Ave, New York, NY 10065; e-mail: lyw2001@med.cornell.edu.

References

1. Lenz G, Staudt LM. Aggressive lymphomas. *N Engl J Med*. 2010;362(15):1417-1429.
2. Kurosaki T, Shinohara H, Baba Y. B cell signaling and fate decision. *Annu Rev Immunol*. 2010;28:21-55.
3. Dal Porto JM, Gauld SB, Merrell KT, Mills D, Pugh-Bernard AE, Cambria J. B cell antigen receptor signaling 101. *Mol Immunol*. 2004;41(6-7):599-613.
4. Alizadeh AA, Eisen MB, Davis RE, et al. Distinct types of diffuse large B-cell lymphoma identified by gene expression profiling. *Nature*. 2000;403(6769):503-511.
5. Monti S, Savage KJ, Kutok JL, et al. Molecular profiling of diffuse large B-cell lymphoma identifies robust subtypes including one characterized by host inflammatory response. *Blood*. 2005;105(5):1851-1861.
6. Yang C, Lu P, Lee FY, et al. Tyrosine kinase inhibition in diffuse large B-cell lymphoma: molecular basis for antitumor activity and drug resistance of dasatinib. *Leukemia*. 2008;22(9):1755-1766.
7. Davis RE, Ngo VN, Lenz G, et al. Chronic active B-cell-receptor signalling in diffuse large B-cell lymphoma. *Nature*. 2010;463(7277):88-92.
8. Geahlen RL. Syk and pTyr^d: signaling through the B cell antigen receptor. *Biochim Biophys Acta*. 2009;1793(7):1115-1127.
9. Chen L, Monti S, Juszczynski P, et al. SYK-dependent tonic B-cell receptor signaling is a rational treatment target in diffuse large B-cell lymphoma. *Blood*. 2008;111(4):2230-2237.
10. Friedberg JW, Sharman J, Sweetenham J, et al. Inhibition of Syk with fostamatinib disodium has significant clinical activity in non-Hodgkin lymphoma and chronic lymphocytic leukemia. *Blood*. 2010;115(13):2578-2585.
11. Braselmann S, Taylor V, Zhao H, et al. R406, an orally available spleen tyrosine kinase inhibitor blocks fc receptor signaling and reduces immune complex-mediated inflammation. *J Pharmacol Exp Ther*. 2006;319(3):998-1008.
12. Quiroga MP, Balakrishnan K, Kurtova AV, et al. B-cell antigen receptor signaling enhances chronic lymphocytic leukemia cell migration and survival: specific targeting with a novel spleen tyrosine kinase inhibitor, R406. *Blood*. 2009;114(5):1029-1037.
13. Jo SH, Yang C, Miao Q, et al. Peroxisome proliferator-activated receptor gamma promotes lymphocyte survival through its actions on cellular metabolic activities. *J Immunol*. 2006;177(6):3737-3745.
14. Yang C, Jo SH, Csernus B, et al. Activation of peroxisome proliferator-activated receptor gamma contributes to the survival of T lymphoma cells by affecting cellular metabolism. *Am J Pathol*. 2007;170(2):722-732.
15. Cheng S, Hsia CY, Feng B, et al. BCR-mediated apoptosis associated with negative selection of immature B cells is selectively dependent on Pten. *Cell Res*. 2009;19(2):196-207.
16. Ding BB, Yu JJ, Yu RY, et al. Constitutively activated STAT3 promotes cell proliferation and survival in the activated B-cell subtype of diffuse large B-cell lymphomas. *Blood*. 2008;111(3):1515-1523.
17. Song Z, Lu P, Furman RR, et al. Activities of SYK and PLCgamma2 predict apoptotic response of CLL cells to SRC tyrosine kinase inhibitor dasatinib. *Clin Cancer Res*. 2010;16(2):587-599.
18. Hans CP, Weisenburger DD, Greiner TC, et al. Confirmation of the molecular classification of diffuse large B-cell lymphoma by immunohistochemistry using a tissue microarray. *Blood*. 2004;103(1):275-282.
19. Choi WW, Weisenburger DD, Greiner TC, et al. A new immunostain algorithm classifies diffuse large B-cell lymphoma into molecular subtypes with high accuracy. *Clin Cancer Res*. 2009;15(17):5494-5502.

20. Reilly MP, Sinha U, Andre P, et al. PRT-060318, a novel Syk inhibitor, prevents heparin-induced thrombocytopenia and thrombosis in a transgenic mouse model. *Blood*. 2011;117(7):2241-2246.
21. Bantscheff M, Eberhard D, Abraham Y, et al. Quantitative chemical proteomics reveals mechanisms of action of clinical ABL kinase inhibitors. *Nat Biotechnol*. 2007;25(9):1035-1044.
22. Yokozeki T, Adler K, Lankar D, Bonnerot C. B cell receptor-mediated Syk-independent activation of phosphatidylinositol 3-kinase, Ras, and mitogen-activated protein kinase pathways. *J Immunol*. 2003;171(3):1328-1335.
23. Lenz G, Davis RE, Ngo VN, et al. Oncogenic CARD11 mutations in human diffuse large B cell lymphoma. *Science*. 2008;319(5870):1676-1679.
24. Juszczynski P, Chen L, O'Donnell E, et al. BCL6 modulates tonic BCR signaling in diffuse large B-cell lymphomas by repressing the SYK phosphatase, PTPROT. *Blood*. 2009;114(26):5315-5321.
25. Polo JM, Juszczynski P, Monti S, et al. Transcriptional signature with differential expression of BCL6 target genes accurately identifies BCL6-dependent diffuse large B cell lymphomas. *Proc Natl Acad Sci U S A*. 2007;104(9):3207-3212.
26. Cerchetti LC, Yang SN, Shaknovich R, et al. A peptomimetic inhibitor of BCL6 with potent anti-lymphoma effects in vitro and in vivo. *Blood*. 2009;113(15):3397-3405.
27. Ngo VN, Young RM, Schmitz R, et al. Oncogenically active MYD88 mutations in human lymphoma. *Nature*. 2011;470(7332):115-119.